ChemComm

RSC Publishing

COMMUNICATION

View Article Online
View Journal

Formation and helicity control of ssDNA templated porphyrin nanoassemblies†

Cite this: DOI: 10.1039/c2cc38150h

Received 12th November 2012,
Accepted 14th December 2012

DOI: 10.1039/c2cc38150h

www.rsc.org/chemcomm

Gevorg Sargsyan, Alexandra A. Schatz, Jan Kubelka and Milan Balaz*

We report the formation of left- (M-helix) and right-handed (P-helix) nanoassemblies of a porphyrin–diaminopurine conjugate (Por–DAP) templated by a single stranded oligodeoxythymidine (dT40) *via* directional hydrogen bonding. The supramolecular helicity can be controlled by the ionic strength, Por–DAP : dT40 ratio, and annealing rate.

The importance of chirality in nature is well pronounced by the preferred handedness and the existence of single enantiomers of essential biomolecules. Chiral nanostructures have a great potential for applications in chiroptical devices. For example, chiral nematic fluids demonstrated distinct light reflecting properties depending on the pitch and the sense of helical components.[1,2] DNA is one of the most frequently employed chiral nano-frameworks. Particularly, its molecular structure can be easily transformed into helical periodically patterned multi-chromophoric ladders. Porphyrins found widespread applications as building blocks in functional nanoarchitectures.[3–13] The majority of non-covalent porphyrin–DNA assemblies rely on stacking and electrostatic interactions between charged porphyrins and the oligodeoxynucleotide (ODN) duplex. These non-specific interactions, however, do not allow accurate control over the geometry and size of the porphyrin nanoassemblies.[14–18] Templated self-assembly by hydrogen-bond directed molecular recognition provides access to nanostructures of controlled geometry and photophysical properties.[19,20] External stimuli can dictate the structure and arrangement of ODN templated chromophores. However, controlling the helical sense of H-bond templated assembly built on an ODN with a single absolute stereochemistry remains a challenge. So far, only one example of H-bonded DNA-templated multichromophoric nanoassembly with right- and left-handed helicities has been reported.[21] Herein we present left- and right-handed porphyrin nanoladders assembled on oligodeoxythymidine *via* directional H-bonding.

Department of Chemistry, University of Wyoming, 1000 E. University Avenue, Laramie, WY 82071, USA. E-mail: mbalaz@uwyo.edu

† Electronic supplementary information (ESI) available: Experimental conditions, UV-vis, fluorescence, CD, resonance light scattering spectra, TEM micrographs of **Por–DAP**·**dT40** nanoassemblies, and density functional theory (DFT) simulations. See DOI: 10.1039/c2cc38150h

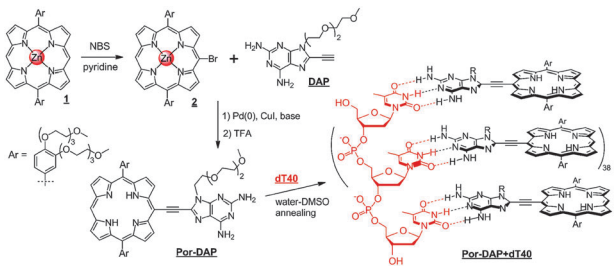

Scheme 1 Synthesis of porphyrin–diaminopurine conjugate **Por–DAP** and its self-assembly on oligothymine 5′-$(dT)_{40}$ template **dT40** *via* directional H-bonding between diaminopurine and thymidine.

To assemble non-covalent helical stacks of porphyrins along single stranded DNA *via* directional H-bonding, we used the complementary pairing of the diaminopurine with thymidine. The 2,6-diaminopurine has been shown to form three hydrogen bonds with thymine.[22] The 5,15-diarylporphyrin **1** was prepared in one step by acid-catalysed condensation of dipyrromethane with 3-triethyleneglycol substituted benzaldehyde followed by *in situ* oxidation with DDQ and metallation with zinc acetate (Scheme 1 and ESI†).[23] Amphiphilic triethylene glycol side chains were employed to increase the water solubility of the Por–DAP conjugate. Statistical bromination of **1** with NBS gave, after chromatography, mono-*meso*-brominated porphyrin **2**. The triethyleneglycol substituted 8-acetyl-2,6-diaminopurine **DAP** was synthesized in four steps from 2,6-diaminopurine.[21] The palladium-catalyzed Sonogashira cross-coupling between the brominated porphyrin **2** and acetylated diaminopurine **DAP** followed by demetallation with trifluoroacetic acid yielded the porphyrin–diaminopurine conjugate **Por–DAP**.

The non-self-complementary oligodeoxythymine 5′-$(dT)_{40}$ (**dT40**) was selected as a template. Based on the DNA and porphyrin geometries, the assembly is expected to be approximately 13 nm long and 4 nm wide. To explore the assembly of DNA templated **Por–DAP** supramolecular ladders, a solution of **Por–DAP** (10 μM) in DMSO was added to a solution of 5′-$(dT)_{40}$ (**dT40**, 10 μM, nucleobase concentration) in Na-cacodylate buffer (1 mM, pH 7.0) at 85 °C. The DMSO content of the final sample was varied from 10% to 70%.

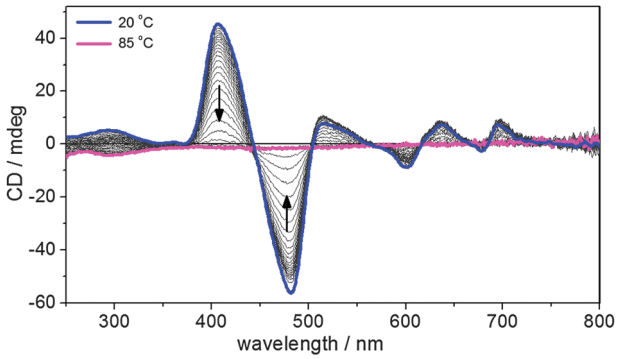

Fig. 1 Variable temperature CD spectra of the **Por–DAP·dT40** nanoassemblies[26] from 20 °C to 85 °C (0.5 °C min^{-1}).

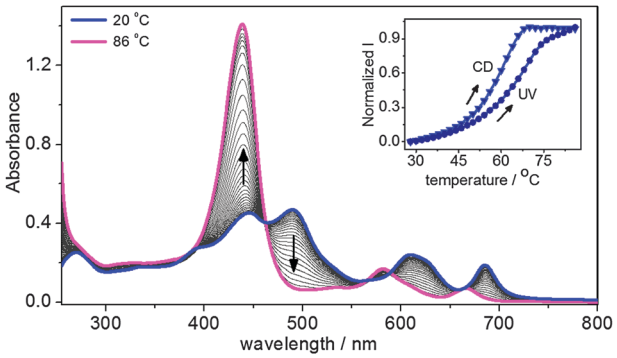

Fig. 2 Variable temperature UV-vis spectra of the **Por–DAP·dT40** nanoassemblies[26] from 20 °C to 85 °C (0.5 °C min^{-1}). Inset: CD (481.5 nm) and absorption (439.0 nm) signals plotted as a function of temperature.

The solution was kept at 85 °C for 1 h to ensure full homogeneity of the sample. No CD signal was observed at 85 °C for any DMSO concentration studied. The solution was then cooled to 20 °C (slow annealing, gradient: −0.5 °C min^{-1}, 1 min equilibration time, cooling time 260 min) to promote the formation of templated **Por–DAP·dT40** assembly *via* hydrogen bond interactions between the **Por–DAP** and **dT40**.[24] The most intense CD spectrum was observed in 40% aqueous DMSO (Fig. 1, blue curve) with negative Cotton effects at 678 nm (−2.6 mdeg), 601 nm (−8.8 mdeg) and 481.5 nm (−56.5 mdeg) and positive Cotton effects at 694 nm (+7.2 mdeg), 637 nm (+7.4 mdeg), 515 nm (+8.0 mdeg), 406 nm (+45.0 mdeg), and 292 nm (+5.2 mdeg). The negative CD couplet observed in the Soret band region arises from the counterclockwise arrangement of porphyrins within the assembly (M-helix).[25] This is confirmed by excellent agreement of the experimental CD with simulations using time-dependent density functional theory (TD-DFT) for a model porphyrin tetramer (see ESI,† Fig. S23 and S24). No CD signal was observed at 20 °C for the samples with $\leq$20% and $\geq$ 50% of DMSO (Fig. S1, ESI†). The CD signal below 240 nm was not monitored because of the DMSO absorption overlap, hence limited data were obtained for the conformation of the DNA strand.

The slow annealing of the **Por–DAP + dT40** mixture from 85 °C to 20 °C revealed a 60% hypochromicity of the Soret band and appearance of a new band at 491.0 nm indicating a columnar stacking of porphyrins (Fig. 2). Analysis of CD and UV-vis melting curves gave melting temperature T_m = 57.3 °C and T_m = 65.3 °C, respectively (Fig. 2, inset). Variable temperature fluorescence and resonance light scattering (RLS) experiments corroborated the CD and UV-vis results (Fig. S3–S10, ESI†). Annealing of **Por–DAP** with a non-complementary oligoadenosine (**dA40**) did not yield an induced CD signal (Fig. S11, ESI†).

Next we explored the effect of ionic strength on the helicity of the **Por–DAP·dT40** assembly. The CD spectrum of the **Por–DAP·dT40** nanoassemblies formed by slow annealing in the presence of 500 mM NaCl yielded a nearly mirror-imaged CD profile (Fig. 3, red curve) compared to the assemblies formed in the absence of NaCl (M-helix, Fig. 3, blue curve). The virtually inverted CD signal is strong evidence of helicity inversion of **Por–DAP·dT40**. Post-assembly removal of NaCl from the solution by dialysis did not have any effect on the CD spectrum of **Por–DAP·dT40** nanoassemblies (Fig. S25, ESI†). TD-DFT calculations of the CD

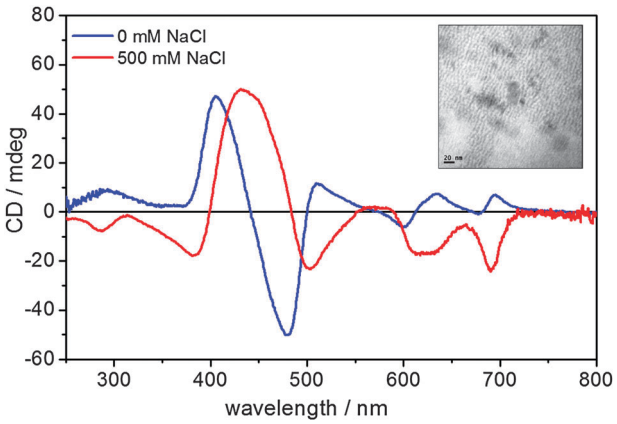

Fig. 3 CD spectra of the **Por–DAP·dT40** nanoassemblies formed by slow cooling in the absence (blue curve, M-helix) and presence (500 mM, P-helix, red curve) of NaCl.[26] Inset: TEM image of **Por–DAP·dT40** nanoassemblies formed in the presence of NaCl (scale bar = 20 nm).

for model clockwise **Por–DAP** arrangements are consistent with the observed spectral sign patterns (Fig. S24, ESI†). Lastly, TEM images of a solution of **Por–DAP·dT40** assembled in the presence of 500 mM NaCl revealed structures with lengths of 8–16 nm and a width of 4–6 nm, both within theoretically predicted values (Fig. S18, ESI†).

The molar fraction of **Por–DAP–dT40** as well as the annealing rate of the sample had a strong effect on the helicity of **Por–DAP·dT40** (Fig. 4). Various concentrations of **Por–DAP** and **dT40** were mixed at 85 °C in the presence of NaCl, while the total concentration of **dT40** and **Por–DAP** was kept constant (20 μM), followed by slow annealing (Fig. S13, ESI†). The annealing of **Por–DAP** (4 μM) with **dT40** (16 μM) in the presence of 500 mM NaCl gave rise to a CD spectrum of opposite sign though of smaller intensity (Fig. 4a, green curve) compared to annealing of the 10 + 10 μM **Por–DAP–dT40** mixture (Fig. 4a, red line).

To evaluate the effect of annealing rate on **Por–DAP·dT40** helicity, we compared two different cooling rates, (i) slow annealing reported in the above, and (ii) a fast annealing with a cooling time of <5 min (inset, Fig. 4b). For the latter, a sample heated to 85 °C was quickly placed in a holder pre-equilibrated at 20 °C. Even though the sample temperature dropped from 85 °C to 22 °C in 4 minutes, it took

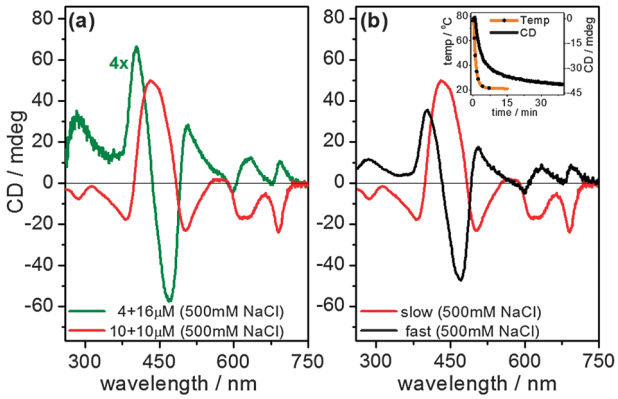

Fig. 4 CD spectra of the **Por–DAP·dT40** nanoassemblies formed by (a) slow annealing at various molar ratios of **Por–DAP** and **dT40** in the presence of NaCl; and (b) by fast (black curve) and slow (red curve) annealing of **Por–DAP** (10 μM) and **dT40** (10 μM) in the presence of 500 mM NaCl. Inset: plot of temperature (orange curve) and CD signal (480 nm, black curve) as a function of time (fast annealing, 500 mM NaCl).

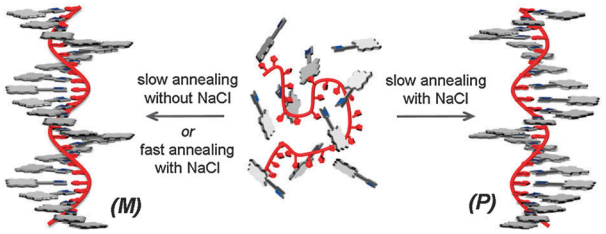

Fig. 5 Schematic illustration of the formation of left-handed (M) and right-handed (P) **Por–DAP·dT40** nanoassemblies.

approximately 50 minutes for the assembly to form based on the CD signal (Fig. 4, inset). The increase of the negative CD signal at 480 nm followed a biexponential decay with t_1 = 50.7 min and t_2 = 3.6 min. The fast cooling experiment revealed the formation of M-assemblies with a virtually mirror image CD spectrum compared to slow annealing in the presence of 500 mM NaCl (Fig. 4b). The cooling rates had a small effect on helicity of **Por–DAP·dT40** assemblies formed in the absence of NaCl (Fig. S14, ESI†). Slow or fast annealing of **Por–DAP** with **dA40** in the presence of NaCl did not yield an induced CD signal (Fig. S11, ESI†). Two opposite helicities were thus easily obtained by changing the annealing rate in the presence of 500 mM NaCl.

In conclusion, we have shown that achiral porphyrin–diaminopurine conjugate **Por–DAP** can be assembled into right- and left-handed nanoladders of a defined size *via* directional hydrogen bonding using oligodeoxythymine **dT40** as a template (Fig. 5). UV-vis absorption, fluorescence, and RLS data together with TEM corroborated the formation of DNA templated porphyrin nanoassemblies. The handedness of **Por–DAP·dT40** nanoassemblies could be controlled by the ionic strength, chromophore–template molar ratio, and the annealing rate. This is the first example where helicity of porphyrin nanoarrays templated on ssDNA *via* directional H-bonding was controlled and switched by environmental conditions. We believe that these highly modular systems have excellent potential to be utilized in chiral memory and chirophotonic applications.

The work was supported by the UW Start-up Funds, School of Energy Resources Graduate Assistantship (G.S.), UW REU program (A.A.S) and NSF Career 0846140 (J.K.). We thank F. Ngwa and Prof. B. Leonard (UW).

Notes and references

1 D. J. Broer, C. M. W. Bastiaansen, M. G. Debije and A. P. H. J. Schenning, *Angew. Chem., Int. Ed.*, 2012, **51**, 7102–7109.
2 Y. Wang and Q. Li, *Adv. Mater.*, 2012, **24**, 1926–1945.
3 T. S. Balaban, N. Berova, C. M. Drain, R. Hauschild, X. F. Huang, H. Kalt, S. Lebedkin, J. M. Lehn, F. Nifaitis, G. Pescitelli, V. I. Prokhorenko, G. Riedel, G. Smeureanu and J. Zeller, *Chem.–Eur. J.*, 2007, **13**, 8411–8427.
4 M. De Napoli, S. Nardis, R. Paolesse, M. G. H. Vicente, R. Lauceri and R. Purrello, *J. Am. Chem. Soc.*, 2004, **126**, 5934–5935.
5 *Synthesis and applications of supramolecular porphyrinic materials*, in *Functional Molecular Nanostructures*, ed. C. M. Drain, I. Goldberg, I. Sylvain and A. Falber, Berlin, 2005, pp. 55–88.
6 L. A. Fendt, I. Bouamaied, S. Thoni, N. Amiot and E. Stulz, *J. Am. Chem. Soc.*, 2007, **129**, 15319–15329.
7 M. Hoffmann, J. Kärnbratt, M.-H. Chang, L. M. Herz, B. Albinsson and H. L. Anderson, *Angew. Chem., Int. Ed.*, 2008, **47**, 4993–4996.
8 M. Jurow, A. E. Schuckman, J. D. Batteas and C. M. Drain, *Coord. Chem. Rev.*, 2010, **254**, 2297–2310.
9 E. Maligaspe, N. V. Tkachenko, N. K. Subbaiyan, R. Chitta, M. E. Zandler, H. Lemmetyinen and F. D'Souza, *J. Phys. Chem. A*, 2009, **113**, 8478–8489.
10 T. Nguyen, A. Brewer and E. Stulz, *Angew. Chem., Int. Ed.*, 2009, **48**, 1974–1977.
11 G. Sargsyan and M. Balaz, *Org. Biomol. Chem.*, 2012, **10**, 5533–5540.
12 A. Satake and Y. Kobuke, *Org. Biomol. Chem.*, 2007, **5**, 1679–1691.
13 A. W. I. Stephenson, A. C. Partridge and V. V. Filichev, *Chem.–Eur. J.*, 2011, **17**, 6227–6238.
14 A. D'Urso, A. Mammana, M. Balaz, A. E. Holmes, N. Berova, R. Lauceri and R. Purrello, *J. Am. Chem. Soc.*, 2009, **131**, 2046–2047.
15 R. Lauceri, R. Purrello, S. J. Shetty and M. G. H. Vicente, *J. Am. Chem. Soc.*, 2001, **123**, 5835–5836.
16 D. R. McMillin, A. H. Shelton, S. A. Bejune, P. E. Fanwick and R. K. Wall, *Coord. Chem. Rev.*, 2005, **249**, 1451–1459.
17 R. F. Pasternack, *Chirality*, 2003, **15**, 329–332.
18 T. Yamamoto, D. H. Tjahjono, N. Yoshioka and H. Inoue, *Bull. Chem. Soc. Jpn.*, 2003, **76**, 1947–1955.
19 J. L. Sessler, J. Jayawickramarajah, A. Gouloumis, T. Torres, D. M. Guldi, S. Maldonado and K. J. Stevenson, *Chem. Commun.*, 2005, 1892–1894.
20 P. G. A. Janssen, J. Vandenbergh, J. L. J. van Dongen, E. W. Meijer and A. Schenning, *J. Am. Chem. Soc.*, 2007, **129**, 6078–6079.
21 P. G. A. Janssen, A. Ruiz-Carretero, D. González-Rodríguez, E. W. Meijer and A. P. H. J. Schenning, *Angew. Chem., Int. Ed.*, 2009, **48**, 8103–8106.
22 J. Booth, W. J. Cummins and T. Brown, *Chem. Commun.*, 2004, 2208–2209.
23 M. Balaz, H. A. Collins, E. Dahlstedt and H. L. Anderson, *Org. Biomol. Chem.*, 2009, **7**, 874–888.
24 M. M. J. Smulders, A. P. H. J. Schenning and E. W. Meijer, *J. Am. Chem. Soc.*, 2007, **130**, 606–611.
25 N. Berova and K. Nakanishi, Exciton Chirality Method: Principles and Applications, in *Circular Dichroism, Principles and Applications*, ed. N. Berova, K. Nakanishi and R. W. Woody, New York, 2000, pp. 337–382.
26 The **Por–DAP·dT40** nanoassemblies were prepared by cooling the solution of **Por–DAP** (10 μM) and **dT40** (10 μM) from 85 °C to 20 °C (cooling rate: 0.5 °C min^{-1} + 1 min wait). Solvent: 40% DMSO in Na-cacodylate buffer (1 mM, pH = 7.0).